Short communications

Effect of supplied CO-CO$_2$ in the presence of carbon

Lisa Deleebeeck$^{\boxtimes}$ and Kent Kammer Hansen$^{\boxdot}$

Department of Energy Conversion and Storage, Danish Technical University (DTU), Risø Campus, Frederiksborgvej 399, PO BOX 49, DK-4000 Roskilde, Denmark

$^{\boxtimes}$Corresponding Author: ldel@dtu.dk; Tel.: +45-46 77 58 35; $^{\boxdot}$Scientific enquiries: kkha@dtu.dk

Abstract

The effect of varying the CO-CO$_2$ and CO$_2$-N$_2$ ratios was investigated in the presence of coal in a specially designed 3-electrode setup, used to simulate the anode compartment in a hybrid direct carbon fuel cell (HDCFC). The HDCFC consists of a hybrid between a molten carbonate and a solid oxide fuel cell (SOFC). It was shown that the cell performance improved with increased CO$_2$ content in the CO$_2$-N$_2$ mixture, due to the formation of CO from the inverse Boudouard reaction. The same was seen for CO/CO$_2$ gas mixtures in the presence of coal, in contrast to CO-fueled SOFCs.

Keywords
Hybrid direct carbon fuel cell (HDCFC); DCFC; 3-electrode; Half-cell; Cyclic voltammetry (CV); Coal; Carbon monoxide

Introduction

Direct carbon fuel cells (DCFCs) include different types of fuel cells, which may be differentiated by their electrolytes: including molten hydroxide, molten carbonate and solid oxide [1,2]. Solid oxide fuel cell (SOFC)-type DCFCs are identical to gas-fueled (*e.g.* H$_2$, CO) SOFCs, with the addition of carbon loaded into the anode chamber, either in direct contact with the electrolyte, typically yttria-stabilized zirconia (YSZ), or with an anode layer (*e.g.* Ni-YSZ). Carbon sources may include carbon black, graphite, coals or various types of biomass [3]. Due to the solid nature of the fuel and the electrolyte, the electrochemically active contact area is relatively limited in SOFC-type DCFCs. To partially overcome this limitation, molten slurries containing dispersed carbon are introduced into the anode chamber. Molten materials include metals [4] or alkali carbonates (e.g., (Li-K)$_2$CO$_3$), where the latter is termed a hybrid direct carbon fuel cell (HDCFC) as it is a hybrid between molten carbonate (MCFC) and SOFCs [2].

Several reports in the literature have previously dealt with gas-fueled SOFC performance at various $CO:CO_2$ ratios, focusing primarily on different anode/fuel-electrode materials, including Ni-YSZ [5,6], gadolina-doped ceria (GDC) [7], $La_{1-x}Sr_xCr_{1-y}Mn_yO_{3\pm\delta}$ (LSMC) and Pt-(Ce, Y, Zr)$O_{2-\delta}$ [8]. When operating in fuel- [9] or electrolyzer-cell [5] modes, the deposition of carbon is undesirable in these systems, as this leads to decreased electrochemical activity, and destruction of Ni-YSZ electrodes due to carbon dusting of Ni. In the case of DCFCs, carbon is purposefully loaded into the anode chamber to serve as a source of fuel. In this investigation, we explore the effects of variable $CO:CO_2$ ratio on fuel cell performance of a Ni-YSZ anode in the presence, and absence (CO-fueled SOFC), of carbon fuel (treated anthracite and bituminous coals, SOFC-type DCFC) and mixed carbon-carbonate (HDCFC). Although such a combination of fuels (solid carbon and $CO_{(g)}$) is unlikely in technological applications, these investigations aid in the understanding of the chemical reactions occurring in the vicinity of the anode within the carbon-molten carbonate slurry of a HDCFC.

Experimental

Three types of coal were acquired from INCAR (Spain): milled and demineralised bituminous (Coal I) [10], carbonized, milled and demineralised anthracite (Coal II) and milled bituminous coal (Coal III). Coals were combined, as received, with (62-38 wt% Li-K)$_2CO_3$ (CO3) (4:1 wt% C:CO3) and ball milled dry for 3 h. Mixed coal-carbonate, carbonate and B-II coal alone were loaded into a zirconia tube sealed onto a 3-electrode (3E) YSZ pellets developed at DTU-Risø [11,12], equipped with a Au mesh at the Ni-YSZ working electrode (WE, 7.4 mm diameter), and Pt counter (CE) and reference electrodes (RE), as described in Deleebeeck and Hansen [13], and shown schematically in Figure 1.
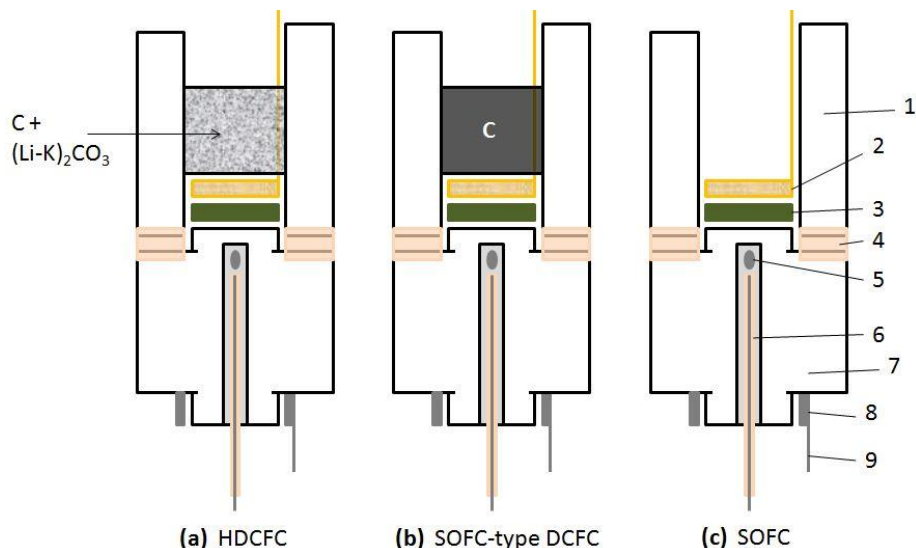

Figure 1. Three-electrode half-cell electrochemical setup, illustrated as cross-sections, with (a) carbon and carbonate (HDCFC configuration) and (b) carbon (SOFC-type DCFC configuration) loaded at the WE, as well as (c) without solid carbon fuel (gaseous-fueled SOFC configuration). Where 1 = zirconia tube, 2 = WE current collector (Au), 3 = Ni-YSZ WE layer, 4 = alumina sealant, 5 = RE (Pt), 6 = alumina tube/guide rod, 7 = YSZ pellet, 8 = CE (Pt), and 9 = CE current collector (Pt).

Cells were heated to 800 °C in N_2 (180 °C/h), and held at 800 °C for 30 min. Experiments were carried out between 700 and 800 °C in mixed N_2-CO_2 and CO-CO_2 environments (2.3 L/h total flow rate). Chronopotentiometry was performed to determine open circuit potential (OCP) by holding

current fixed at 0 mA for 5 min. OCP was determined by combining potential measured during chronopotentiometry (galvanostatic measurement) with pO_2 sensor data acquired simultaneously, such that OCP values are reported as absolute values *vs.* Pt/air. Cyclic voltammetry (CV) was acquired between ± 500 mV *vs.* internal RE (Pt/CO-CO_2, termed 'potential difference', ΔE) at 10 mV/s (3 replicate cycles). From CV measurements, current, reported in mA, was measured at a fixed overpotential (η) of 500 mV *vs.* OCP (Pt/air). The natural logarithm of currents measured at fixed overpotential was plotted versus inverse temperature in Kelvin according to the Arrhenius equation, allowing the calculation of activation energies E_a / eV. Electrochemical impedance spectroscopy (EIS) was acquired between 85,000 and 0.1 Hz (6 pts/decade) with an AC perturbation of 30 mV. Nyquist plots of EIS data were fitted using a model circuit consisting of a series resistance (R_s) in series with two resistor-constant phase element units (RQ, in parallel). Polarization resistance (R_p) was calculated from the sum of the two resistors in series.

Results and discussion

Temperature

Typical CV data acquired in the presence of carbonate (Li-K)$_2$CO$_3$, Coal III_CO3 and Coal III (only), *i.e.*, without carbonate present, at 800 °C in 96-4 vol% N_2-CO_2 is shown in Figure 2(a). These CVs illustrate the various types of direct carbon/coal fuel cell (DCFC) performance investigation, including a SOFC-type DCFC [1] with only carbon (Coal III) present at the WE (Figure 1(b)), and a HDCFC [2] with mixed carbon-carbonate (Coal III_CO3) present (Figure 1(a)) [14-16]. The CV acquired in molten carbonate 62-38 wt% (Li-K)$_2$CO$_3$ represents the potential cycling of the Ni-YSZ anode in a molten carbonate environment, and is included to illustrate the difference versus a HDCFC [17].

As seen in Figure 2(a), SOFC-type DCFC performance was relatively limited due the finite contact between solid carbon and the WE. HDCFC performance was greater due to the extended contact between the carbon fuel and electrolyte, as expanded by the molten carbonate medium. Further, the CV shape of carbonate and mixed carbon-carbonate are seen to differ significantly. With the exception of Ni-YSZ in molten carbonate, the chemistry in this investigation is expected to be dominated by two processes at the WE: the Boudouard equilibrium (Reaction 1) and the electrochemical oxidation of CO by O^{2-} (Reaction 2) supplied through the YSZ electrolyte or CO_3^{2-} (Reaction 3) [18]. Additionally, reactions occurring at the WE include, amongst others, the decomposition/formation of carbonate (Reaction 4), while CO_2 reduction (reverse of Reaction 2) proceeds at the CE and RE [19].

$$C_{(s)} + CO_2 \leftrightarrow 2CO \tag{1}$$

$$CO + O^{2-} \rightarrow CO_2 + 2e^- \tag{2}$$

$$CO + CO_3^{2-} \rightarrow 2CO_2 + 2e^- \tag{3}$$

$$CO_3^{2-} \leftrightarrow O^{2-} + CO_2 \tag{4}$$

Current was measured at a fixed overpotential (η) of 500 mV (*vs.* OCP), as illustrated in Figure 2(a) for Coal III_CO3, between 700 and 800 °C in 96-4 N_2-CO_2, and are plotted according to the Arrhenius equation in Figure 2(b). SOFC-type DCFC (Coal III (only)) showed activation energy of 2.73 eV, while HDCFC (Coal III_CO3) showed a significantly lower E_a (1.27 eV) under identical conditions, illustrating that addition of molten carbonate significantly facilitated (lower E_a) the oxidation of carbon under these conditions. The presence of the Ni-YSZ anode was not found to

significantly influence the E_a values determined for carbon black in the HDCFC configuration, however, the magnitude of the measured current was significantly reduced [19].
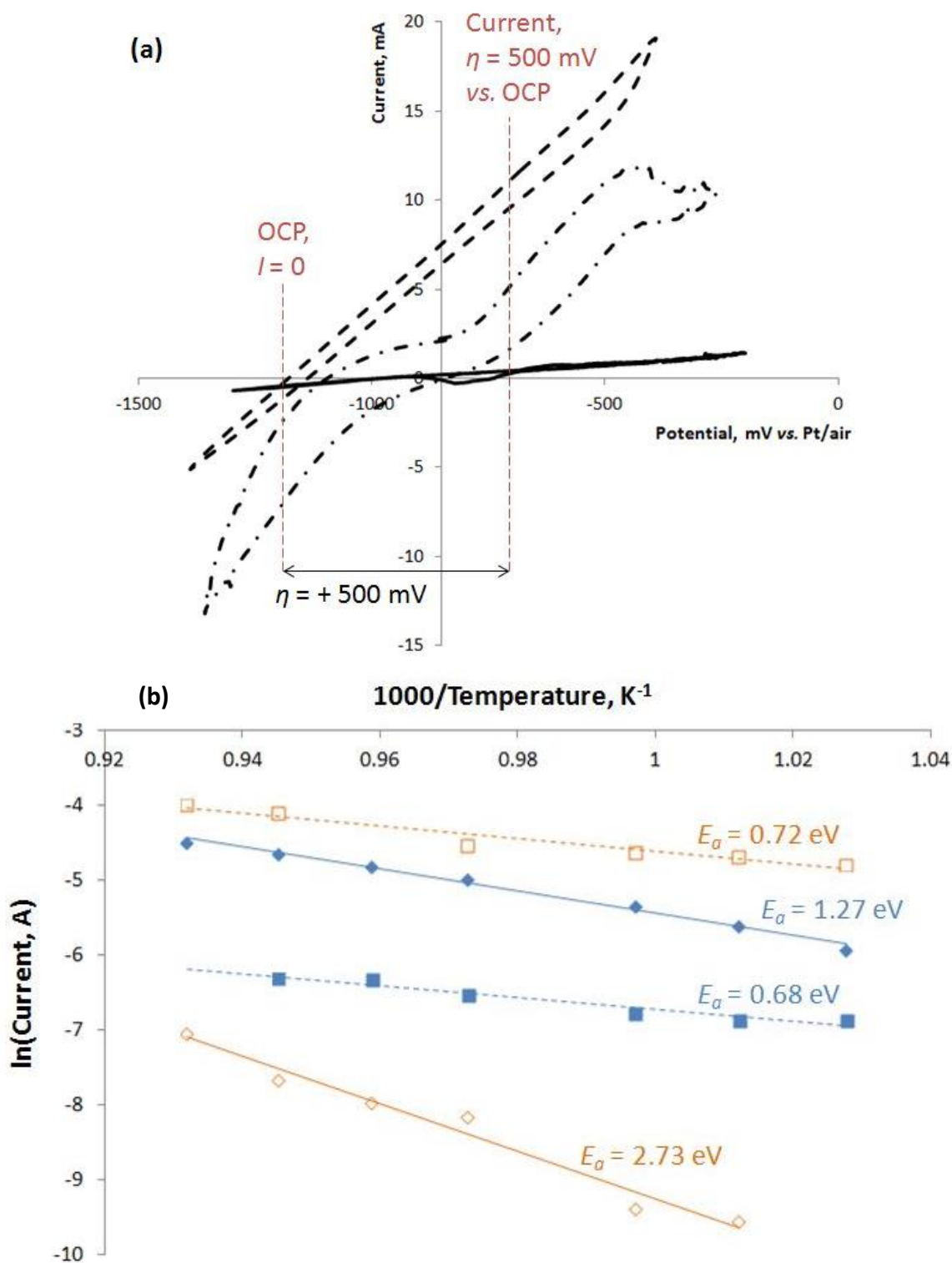

Figure 2. (a) *CV acquired at 800 °C in 96-4 vol % N$_2$-CO$_2$ (6 L/h total flow), plotted as a function of potential for carbonate (Li-K)$_2$CO$_3$ (- · - ·), Coal III + CO3 (Coal III_CO3, - - - -) and Coal III (only) (----) loaded at the WE of a 3E half-cell.*
(b) *Arrhenius plot of Coal III_CO3 (closed symbols) in 96-4 vol% N$_2$-CO$_2$ (◊, acting as a HDCFC) and 50-50 vol% CO-CO$_2$ (□), and Coal III (only) (open symbols) in 96-4 vol% N$_2$-CO$_2$ (◊, acting as an SOFC-type DCFC) and 50-50 vol% CO-CO$_2$ (□).*

Activation energies were calculated for both systems (Coal III_CO3 and Coal III (only)) in 50-50 vol% CO-CO_2, giving similar values (0.68 and 0.72 eV, respectively), suggesting that reaction(s) were dominated by the oxidation of CO in both cases. These experiments [13,18,19] do not allow the distinction between oxidants (CO_3^{2-} and O^{2-}), such that the primary electrochemical reaction(s) may include Reactions 2, 3 or both. These activation energy values are slightly lower than those determined on patterned Ni (on YSZ) electrodes (0.85-1.42 eV) [20], but are within the range calculated (0.43-1.64 eV), depending on the rate determining step (RDS), for CO oxidation on Ni-YSZ [21]. Previous side-by-side comparisons of CO-fueled and carbon-loaded SOFCs have included dry CO *vs.* Fe-loaded activated carbon over a Cu/CeO_2 anode between 700 and 850 °C [22] and over a Ag/GDC anode ($(La,Sr)(Ga,Mg)O_{3-\delta}$ electrolyte) at 850 °C [23], coconut carbon-charcoal over a Ag-impregnated Ni-YSZ anode under various sweep gases (He, 8.6 vol% CO_2-He, and 7.4 vol% CO-He) at 750 °C [24], and 92-8 and 50-50 vol% CO-CO_2 vs. lignite coal over a Ni-YSZ/Ni-GDC anode between 750 and 850 °C [25]. Previous studies [22-25] have been carried out in full-cell configurations.

Variable CO_2 content

For each sample, temperature was fixed and content of CO_2 varied in mixed N_2-CO_2 and CO-CO_2 environments. Typical results, including OCP and currents measured at fixed overpotential, in N_2-CO_2 are shown for Coal I_CO3 (770 °C), Coal II_CO3 (770 °C) and Coal III_CO3 (755 °C) in Figures 3-5. In all cases, OCP was seen to decrease as content of CO_2 increased, as expected, due to the inverse relationship between electrochemical potential (E(V)) and the partial pressure of CO_2 (p_{CO2}) in the Nernst Equation (Equation 5) for the oxidation of CO (Reactions 2-3). Current measured at fixed overpotential was seen to increase (Coal I_CO3 and Coal III_CO3) or remain essentially constant (Coal II_CO3) as content of CO_2 increased in mixed N_2-CO_2, as we have shown previously for carbon black [13]. Electrochemical performance, expressed as current at fixed overpotential, varied being coal samples according to source coal characteristics, with bituminous coal (Coals I and III) with lower degree of crystallinity (less graphitic nature) and higher oxygen to carbon content ratios generally showing higher activity. Single-atmosphere half-cell performance as a function of carbon fuel characteristics is discussed in more detail in [19]. As more CO_2 was supplied to the carbon bed, the inverse Boudouard reaction (Reaction 1) produced CO, which was subsequently electrochemically oxidized, generating current under load (*E* > OCP). Activation (increased current under load) as content of CO_2 increased was also seen in EIS data, where R_p decreased (activity increased) with content of CO_2 in N_2-CO_2. Figure 3(d) further illustrates that R_s was largely unaffected by variation in content of CO_2.

$$E = E^0 - \frac{RT}{2F} ln\left(\frac{p_{CO}}{p_{CO_2}}\right) \tag{5}$$

In Equation 5, E^0 and *E* are the standard and measured potentials (mV *vs.* Pt/air), *R* the ideal gas constant, *F* is Faraday's constant, *T* is temperature in Kelvin, and p_{CO} and p_{CO2} are the partial pressures of CO and CO_2, respectively, where p_{CO} + p_{CO2} = 1 atm. It should be noted that OCP is a function of p_{CO} and p_{CO2} in the pore volume of the Ni-YSZ WE, which may differ significantly from the introduced gaseous atmosphere [15, 16]. Especially p_{CO} will vary as a function of experimental variables, including its relative rates of formation through the Boudouard reaction (Reaction 1) and consumption through electrochemical oxidation (Reactions 2 and 3). The Boudouard reaction will depend on temperature, p_{CO2}, and the reactivity of carbon. While solid carbon is typically

ascribed an activity of one, which is assumed to remain unchanged with time, carbon reactivity will depend on its characteristics: degree of crystallinity/graphitic nature, surface area, pore volume, concentration and type of surface groups and hetero-atoms, presence of catalytic/inhibiting impurities, *etc.* [19].
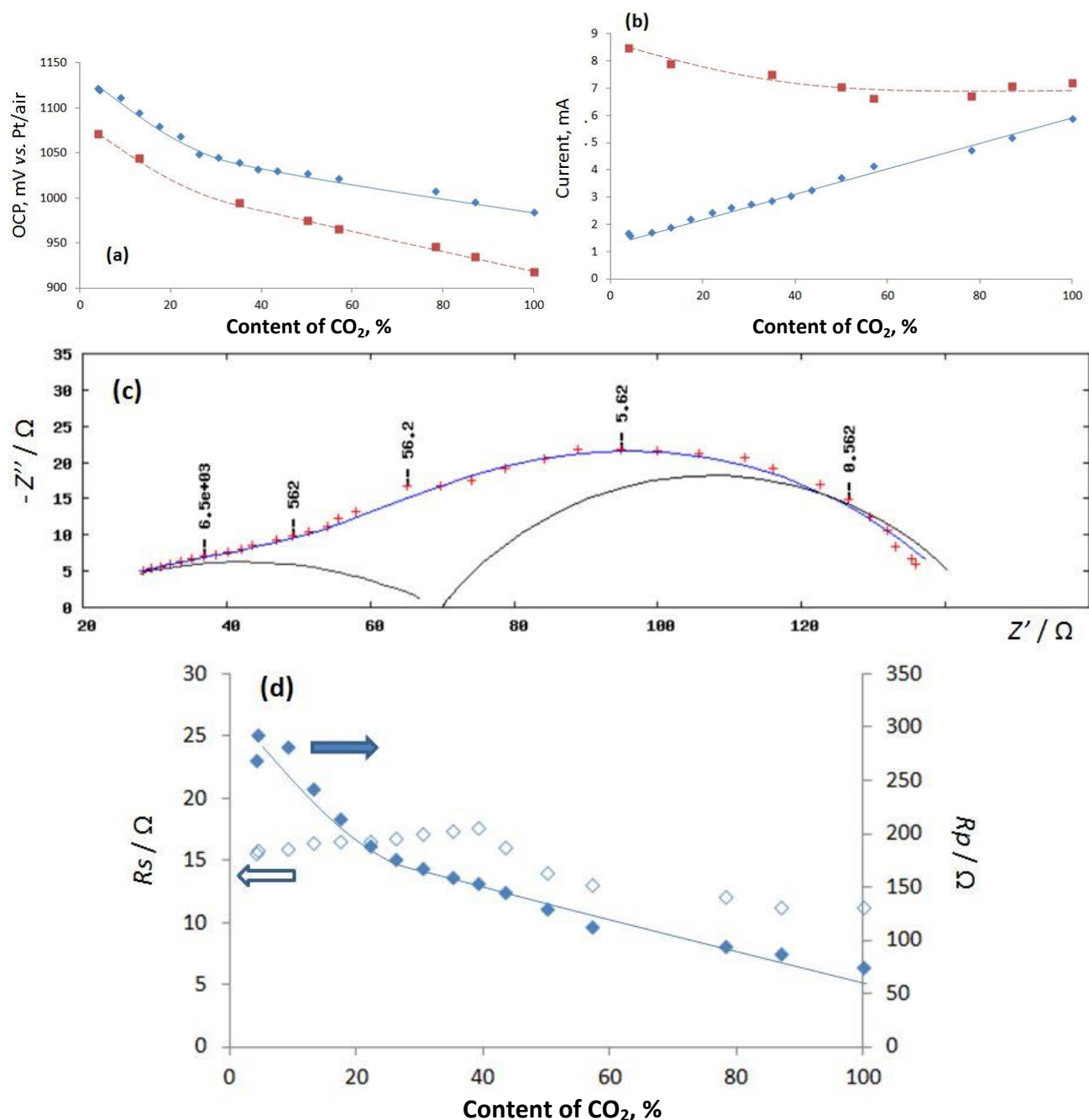

Figure 3. Milled and demineralised bituminous coal (Coal I_CO3) at 770 °C. (a) OCP and (b) current measured at η = 500 mV in N$_2$-CO$_2$ (◊) and CO-CO$_2$ (□). (c) Typical Nyquist plot acquired at 770 °C in 50-50 vol% N$_2$-CO$_2$, where points represent acquired data, curves represent the fit of the model circuit (Rs-RQ-RQ), and frequencies are given in Hz. (d) Rs (open symbols) and R$_p$ (closed symbols) as a function of content of CO$_2$ in N$_2$-CO$_2$. In (a), (b) and (d), points represent acquired data, while lines are included only as visual aids.

Figures 3-5 illustrate how OCP and current measured at fixed overpotential vary as a function of content of CO$_2$ in CO-CO$_2$. In all cases, OCP is seen to decrease with increasing content of CO$_2$, as in mixed N$_2$-CO$_2$ environments. Decreasing OCP values with increasing CO$_2$ in mixed CO-CO$_2$ is consistent with behavior previously reported in the literature for Ni-YSZ [6,9,26] and GDC anodes [7]. As

seen in Figures 3 and 5, OCP values under identical experimental conditions, such as under 100 % CO_2 may not necessarily coincide, this arises due to changing reactivity of the carbon bed as a function of time [19], such that local p_{CO}/p_{CO2} are non-identical despite the same gaseous atmosphere being introduced. As shown in Figure 3, current under load was seen to decrease with increasing content of CO_2 in CO-CO_2 for Coal I_CO3. As supplied CO was assumed to be the primary electrochemical reactant, decreased content of CO in the supplied gas (CO-CO_2) was ex-pected to result in decreased activity (current at fixed overpotential), with performance dramati-cally reduced in the absence of supplied CO (*i.e.* 100 % CO_2) [26]. However, activity in the presence of Coal I_CO3 remained essentially constant at > 50 % CO_2 in mixed CO-CO_2. This suggested that the inclusion of CO_2 to the reaction gas (supplied CO) allowed for the inverse Boudouard reaction (Reaction 1) to supply CO produced inside the reaction chamber, in the Coal I carbon bed. Supply of internally generated CO kept electrochemical activity from decreasing as externally supplied content of CO was decreased. A similar effect was observed for gas-fueled SOFCs H_2-CO mixtures, where for p_{H2} > 0.5 atm (p_{H2} + p_{CO} = 1 atm) the power density at 800 °C was seen to decrease only slightly, relative to a dry H_2 (p_{H2} = 1 atm) system, with the inclusion of CO. This was suggested to result from the *in-situ* (near the electrode/electrolyte interface) generation of H_2 through the water-gas shift reaction between generated H_2O and CO (H_2O + CO $\leftrightarrow$ H_2 + CO_2) [26].
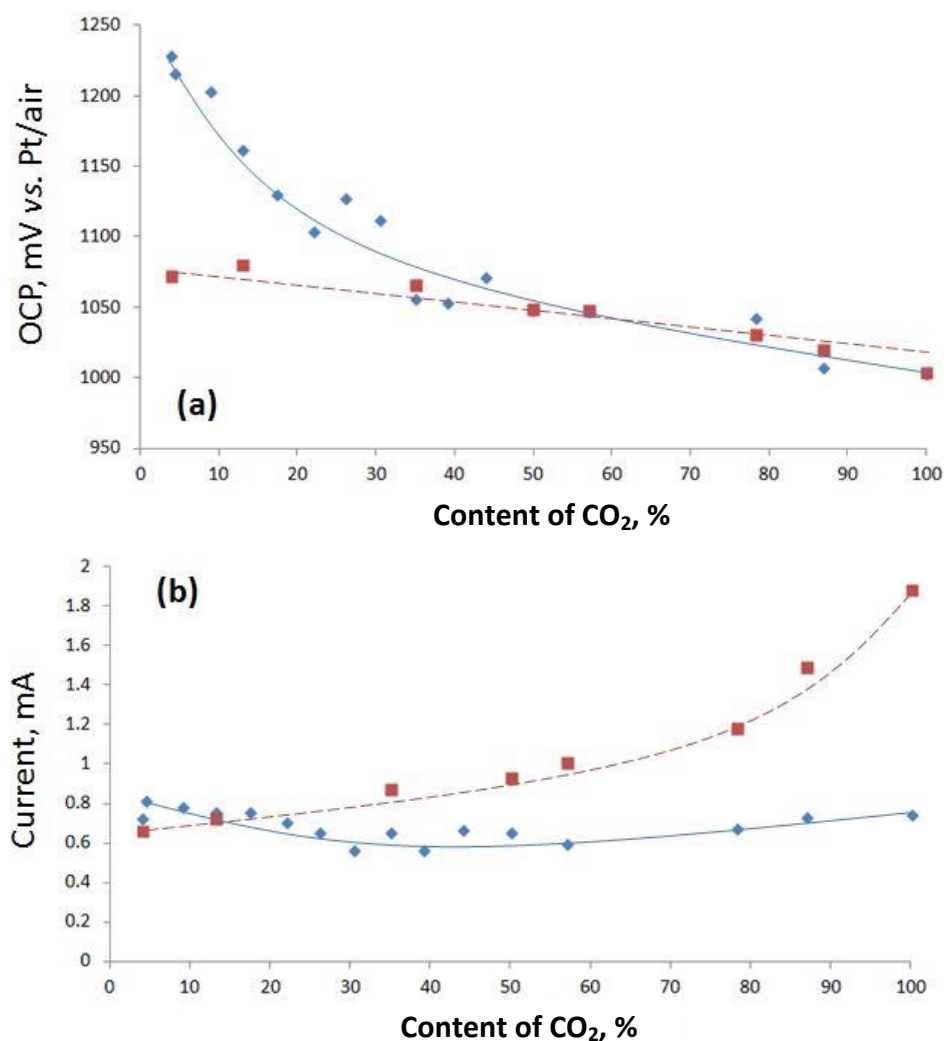

Figure 4. *Carbonized milled and demineralised anthracite (Coal II_CO3) at 770 °C. (a) OCP and (b) current measured at η = 500 mV (overpotential vs. OCP) in N_2-CO_2 (◊) and CO-CO_2 (□).*

For Coal II_CO3 at 770 °C (Figure 4) and Coal III_CO3 at 755 °C (Figure 5), the current at fixed overpotential is seen to increase as content of CO$_2$ increases in mixed CO-CO$_2$. This suggested that even when external CO is supplied (mixed CO-CO$_2$ environment), the enhancement from internally generated CO, illustrated in mixed N$_2$-CO$_2$ as content of CO$_2$ was increased, may be observed. This illustrates the rapid kinetics of the inverse Boudouard reaction (Reaction 1), which is strongly favored at temperatures > 750 °C [1].
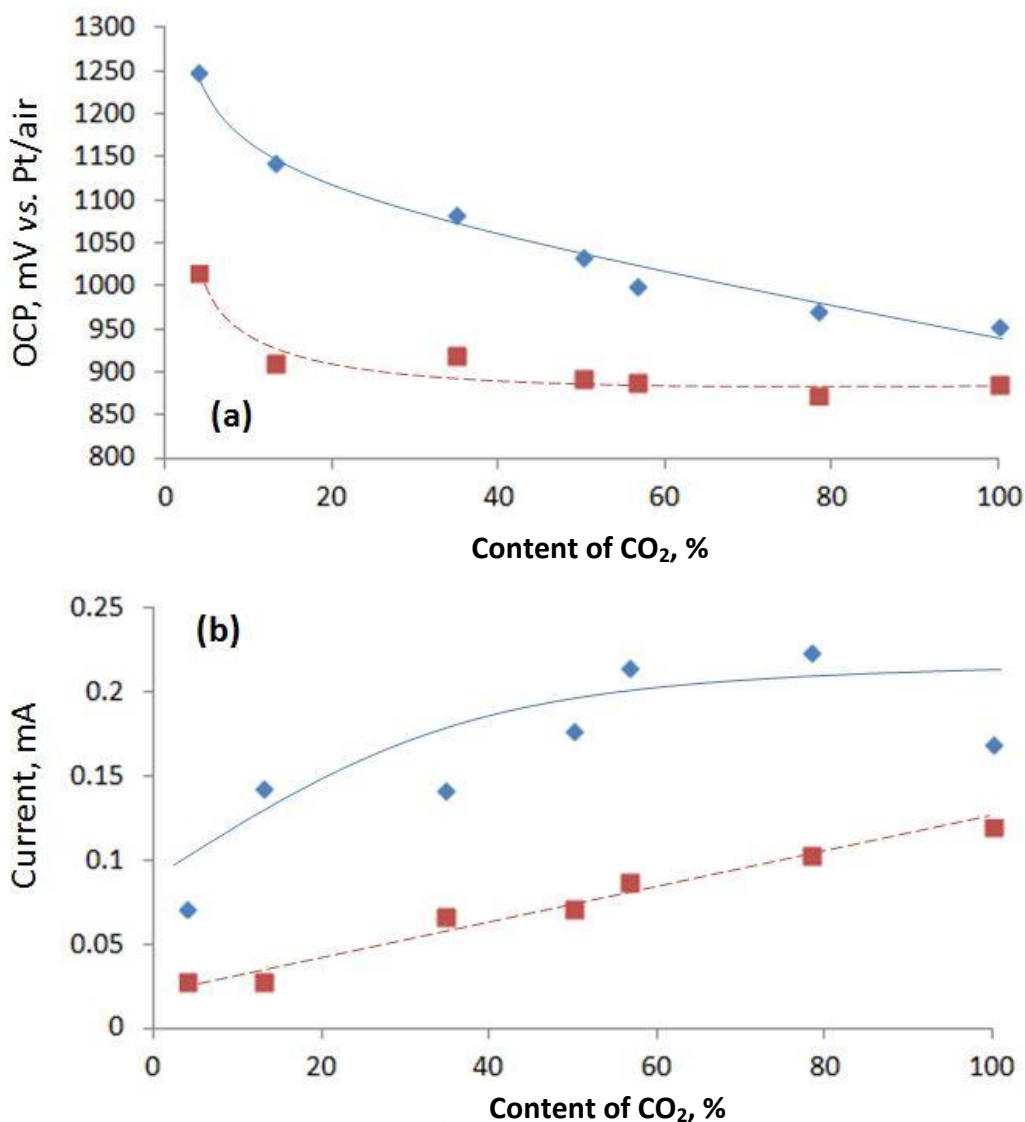
Figure 5. *Milled bituminous coal (Coal III _CO3) at 755 °C. (a) OCP and (b) current measured at η = 500 mV (overpotential vs. OCP) in N$_2$-CO$_2$ (◊) and CO-CO$_2$ (□).*

The increasing cell performance (increased current measured at fixed overpotential) with increasing content of CO$_2$ in CO-CO$_2$ was found to not be limited to HDCFCs. Figure 6 illustrates the same effect in the absence of alkali carbonates, for Coal III (only), at 770 °C in an SOFC-type DCFC configuration (Figure 1(b)). Further, in the absence of carbon, this effect is not seen. When content of CO$_2$ in CO-CO$_2$ was increased for (Li-K)$_2$CO$_3$ alone, in the absence of a solid carbon source, current under load was seen to decrease gradually. In the absence of CO (100 % CO$_2$), current decreased sharply due to fuel starvation conditions. In the absence of both carbon and carbonate, a Ni-YSZ WE (CO-fueled SOFC [11], Figure 1(c)) supplied with progressively lower quantities of CO (increasing content of CO$_2$ in mixed CO-CO$_2$) shows a decrease in activity, as expected [6,26,27].

Interestingly, supplying carbon containing systems with 100 % CO_2 produces lower OCP values, but higher current at fixed overpotential values compared to supplying predominantly CO (96-4 vol% CO-CO_2) (*e.g.* Coal III (only), Figure 6).
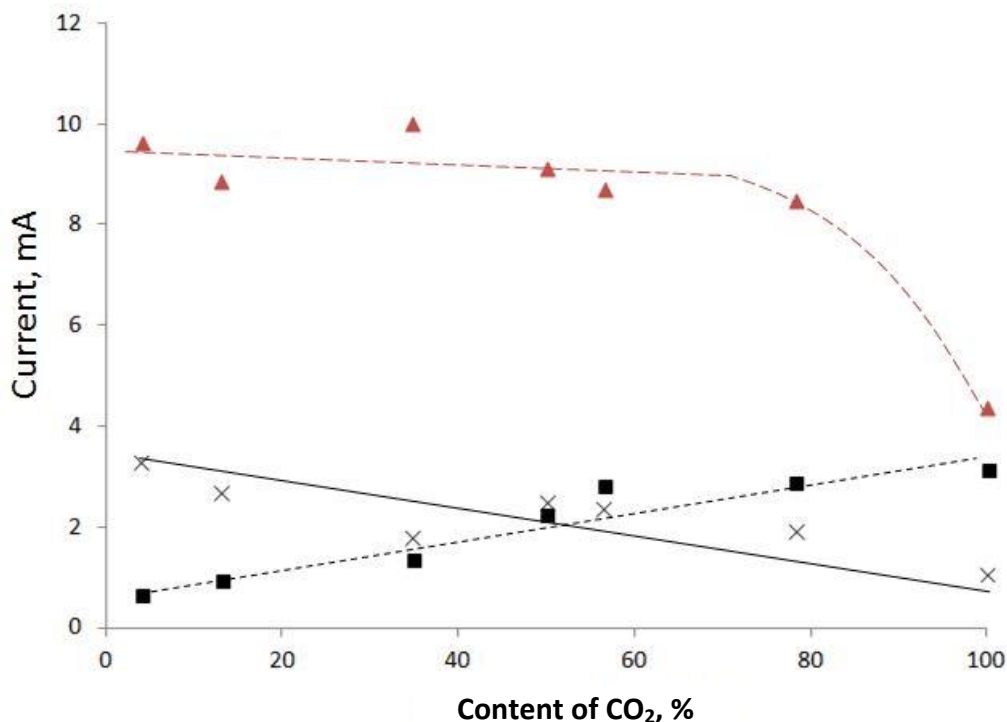

Figure 6. *Current measured at η = 500 mV in CO-CO$_2$ at 770 °C for a Ni-YSZ WE (×), and with milled bituminous coal (Coal III (only), ■) and (Li-K)$_2$CO$_3$ (Δ) at the WE.*

Conclusions

Single-atmosphere 3-electrode electrochemical tests were carried out between 700 and 800 °C in mixed N_2-CO_2 and CO-CO_2 for a Ni-YSZ WE in the presence of molten alkali carbonate $(Li$-$K)_2CO_3$, treated coal (Coal III), and mixed coal-carbonate, including bituminous and anthracite-type coals. Treated coal (Coal III (only)) was tested in a SOFC-type DCFC and mixed coal-carbonates were tested in HDCFC configurations. Activation energies determined in mixed N_2-CO_2 revealed the greater ease of reaction in a mixed carbon-carbonate system.

Half-cell performance was shown, as current measured at fixed overpotential (mV vs. OCP), to increase as content of CO_2 was increased in mixed N_2-CO_2 and CO-CO_2, as supplied CO_2 allowed the generation of CO according to the inverse Boudouard reaction, which was subsequently electrochemically oxidized. In the absence of carbon, with and without (CO-fueled SOFC) carbonates, cell activity was seen to decrease as content of CO_2 in mixed CO-CO_2 was increased, i.e., as the supply of CO was decreased.

References

[1] T. M. Gur, *Chem. Rev*. **113** (2013) 6179-6206, http://pubs.acs.org/doi/abs/10.1021/cr400072b

[2] L. Deleebeeck and K.K. Hansen, *J. Solid State Electrochem*. **18** (2014) 861-882, http://jes.ecsdl.org/content/161/1/F33.short

[3] O. D. Adeniyi and B. C. R. Ewan, Int*. J. Ambient Energy* **33**(4) (2012) 204-208, http://www.tandfonline.com/doi/abs/10.1080/01430750.2012.709357

[4] A. Toleuova, V. Yufit, S. Simons, W. C. Maskell and D. J. L. Brett, *J. Electrochem. Sci. Eng.* **3**(3) (2013) 91-105, http://hrcak.srce.hr/index.php?show=clanak&id_clanak_jezik=162479

[5] S. D. Ebbesen and M. Mogensen, *J. Power Sources* **193** (2009) 349-358, http://www.sciencedirect.com/science/article/pii/S0378775309004686

[6] H. Zhang, J. Chen and J. Zhang, *Int. J. Hydrog. Energy* **38** (2013) 16354-16364, http://www.sciencedirect.com/science/article/pii/S036031991302418X

[7] R. D. Green, C-C. Liu and S. B. Adler, *Solid State Ionics* **179** (2008) 647-660, http://www.sciencedirect.com/science/article/pii/S0167273808003573

[8] F. Bidrawn, G. Kim, G. Corre, J. T. S. Irvine, J. M. Vohs and R. J. Gorte, *Electrochem. Solid St.* **11**(9) (2008) B167-B170, http://esl.ecsdl.org/content/11/9/B167.short

[9] M. Homel, T. M. Gur, J. H. Koh and A. V. Virkar, *J. Power Sources* **195** (2010) 6367-6372, http://www.sciencedirect.com/science/article/pii/S0378775310006464

[10] N. Kaklidis, V. Kyriakou, I. Garagounis, A. Arenillas, J. A. Menendez, G. E. Marnellos and M. Konsolakis, *RSC Adv.* **4** (2014) 18792-18800, http://pubs.rsc.org/EN/content/articlehtml/2014/ra/c4ra01022a?page=search

[11] P. Holtappels, L. G. J. De Haart, U. Stimming, I. C. Vinke and M. Mogensen, *J. Appl. Electrochem.* **29** (1999) 561-568, http://link.springer.com/article/10.1023/A:1003446721350

[12] J. Winkler, P. V. Hendriksen, N. Bonanos and M. Mogensen, *J. Electrochem. Soc.* **145**(4) (1998) 1184-1192, http://jes.ecsdl.org/content/145/4/1184.short

[13] L. Deleebeeck and K. K. Hansen, *Electrochim. Acta* **152** (2015) 222-239, http://www.sciencedirect.com/science/article/pii/S0013468614022725

[14] W. H. A. Peelen, M. Olivry, S. F. Au, J. D. Fehribach and K. Hemmes, *J. Appl. Electrochem.* **30** (2000) 1389-1395, http://link.springer.com/article/10.1023/A:1026586915244

[15] C. C. Chen, T. Maruyama, P. H. Hsieh and J. R. Selman, *ECS Trans.* **28**(30) (2010) 227-239, http://ecst.ecsdl.org/content/28/30/227.short

[16] C. C. Chen, T. Maruyama, P. H. Hsieh and J. R. Selman, *J. Electrochem. Soc.* **159**(10) (2012) D597-D604, http://jes.ecsdl.org/content/159/10/D597.short

[17] J. Liu, K. Ye, J. Zeng, G. Wang, J. Yin and D. Cao, *Electrochem. Commun.* **38** (2014) 12-14, http://www.sciencedirect.com/science/article/pii/S1388248113004189

[18] L. Deleebeeck and K. K. Hansen, *J. Electrochem. Soc.* **161**(1) (2014) F33-F46, http://jes.ecsdl.org/content/161/1/F33.short

[19] L. Deleebeeck, A. Arenillas, J. A. Menendez and K. K. Hansen, *Intl. J. Hydrog. Energy* **40**(4) (2015) 1945-1958, http://www.sciencedirect.com/science/article/pii/S0360319914033473

[20] A. Utz, A. Leonide, A. Weber and E. Ivers-Tiffee, *J. Power Sources* **196** (2011) 7217-7224, http://www.sciencedirect.com/science/article/pii/S0378775310018550

[21] V. Yurkiv, D. Starukhin, H-R. Volpp and W.G. Bessler, *J. Electrochem. Soc.* **158**(1) (2011) B5-B10, http://jes.ecsdl.org/content/158/1/B5.short

[22]   Y. Xie, Y. Tang and J. Liu, *J. Solid St. Electrochem*. **17** (2013) 121-127, http://link.springer.com/article/10.1007/s10008-012-1866-5

[23]   L. Zhang, J. Xiao, Y. Xie, Y. Tang, J. Liu and M. Liu, *J. Alloys Compounds* **608** (2014) 272-277, http://www.sciencedirect.com/science/article/pii/S0925838814009840

[24]   T. Siengchum, F. Guzman and S. S. C. Chuang, *J. Power Sources* **213** (2012) 375-381, http://www.sciencedirect.com/science/article/pii/S0378775312007513

[25]   J. Jewulski, M. Skrzypkiewicz, M. Struzik and I. Lubarska-Radziejewska, *Intl. J. Hydrog. Energy* **39**(36) (2014) 21778-21785, http://dx.doi.org/10.1016/j.ijhydene.2014.05.039

[26]   Y. Jiang and A. V. Virkar, *J. Electrochem. Soc.* **150**(7) (2003) A942-A951, http://jes.ecsdl.org/content/150/7/A942.short

[27]   A. Leonide, S. Hansmann, A. Weber and E. Ivers-Tiffee, *J. Power Sources* **196** (2011) 7343-7346, http://www.sciencedirect.com/science/article/pii/S0378775310018513